

A Mathematical Model to Describe the Melanoma Dynamics under Effects of Macrophage Inhibition and CAR T-cell Therapy

G. RODRIGUES^{1*}, J. G. SILVA², D. S. SANTURIO³ and P. F. A. MANCERA⁴

Received on December 16, 2022 / Accepted on December 26, 2023

ABSTRACT. Melanoma is considered one of the most aggressive types of cancer due to its high propensity for metastasis, which significantly reduces survival chances when detected late. Moreover, melanoma exhibits strong immunogenic characteristics, complicating its treatment, increasing the need to develop more effective techniques of therapy. In the field of oncology, mathematical modeling enables the analysis and distinction of the various mechanisms involved in tumor progression. This allows the analysis of numerous scenarios, which would be impractical experimentally. The main objective of this study is to develop a mathematical model that describes melanoma dynamics in the presence of Tumor-Associated Macrophages (TAM) and Chimeric Antigen Receptor (CAR) T-cell immunotherapy. The goal is to assess why this therapy often falls short in eradicating solid tumors like melanoma and to understand the role of TAM in this failure. This research encompasses stability analysis of the equilibrium points of the model, sensitivity analysis of its parameters, and the examination of numerical solutions. Our results showed that immunosuppression caused by TAM has a negative impact on the effectiveness of the dose and varying the cytotoxicity of CAR T-cells together with dose. Adjusting CAR T-cell cytotoxicity and treatment dosage may enhance tumor control, with the initial tumor burden playing a crucial role in treatment effectiveness.

Keywords: immunotherapy, sensitivity analysis, tumor-associated macrophages.

1 INTRODUCTION

One of the most aggressive types of cancer is the cutaneous melanoma. It is estimated for the year 2023 that there will be about 8,980 new cases of cutaneous melanoma in Brazil [6]. Global projections for new cases of this disease and number of deaths indicate that there will be more

*Corresponding author: Guilherme Rodrigues – E-mail: g.rodrigues2@unesp.br

¹Graduate Programme in Biometrics, IBB/UNESP, 18618-689, Botucatu, SP, Brazil – E-mail: g.rodrigues2@unesp.br – <https://orcid.org/0000-0001-7113-8937>

²Federal Institute of Education, Science and Technology of Mato Grosso, 78600-000, Barra do Garças, MT, Brazil – E-mail: jairo.gomes@ifmt.edu.br – <https://orcid.org/0000-0002-5285-5591>

³National Laboratory of Scientific Computing, 25651-075, Petrópolis, RJ, Brazil – E-mail: danielassanturio@gmail.com – ORCID: <https://orcid.org/0000-0002-6041-5748>

⁴Institute of Biosciences, UNESP, 18618-689, Botucatu, SP, Brazil – E-mail: paulo.mancera@unesp.br – <https://orcid.org/0000-0002-2080-8053>

than 500,000 new cases and approximately 100,000 deaths by 2040 [1]. Melanoma has high resistance to chemotherapy, a fact that compromises the long-term success of treatment, even if it is well targeted. If melanoma is discovered late, the chance of recovery and survival rate decreases dramatically due to its potential to cause metastasis [5].

Adoptive immunotherapy with CAR T-cells has been used as a new strategy to improve cancer treatment, especially for hematological malignancies, with promising results [25]. In addition, several researches involving the use of this therapy against melanoma are ongoing [18,19]. In this therapeutic approach, the patient's T-lymphocytes undergo genetic reprogramming to specifically target antigens expressed on the surface of tumor cells, and upon contact with the malignant cells, the modified T-lymphocyte cells (CAR T-cells) are activated and lead an antitumor immune response [21]. The application of CAR T-cell immunotherapy against melanoma faces several challenges, with the immunosuppressive tumor microenvironment (TME) being a key obstacle to overcome [19].

One of the mechanisms that induce the rapid progression of melanoma is the recruitment of immune system cells. Among all the immune system cells that are mobilized and recruited to tumor sites, macrophages comprise the predominant cellular component within the TME and actively participate in the process of tumorigenesis through a diverse array of molecular pathways and mechanisms. Macrophages that infiltrate solid tumors are called as Tumor-Associated Macrophages (TAM) and participate in tumor progression by secreting growth factors, pro-angiogenic molecules and immunosuppressive factors such as interleukin-10 (IL-10) [8, 10, 17, 20, 23]. Some studies indicate that TAM density in the tumor microenvironment correlates with a poor prognosis of melanoma and acts to prevent the cytotoxic action of T-lymphocytes against tumor cells [3, 20].

Recent publications have emerged in the academic literature, focusing on mathematical models related to CAR T-cells. Eftimie and Hamam [4] investigated the possible mechanisms that could explain the elimination of B16 mouse melanoma cells by immune system cells, such as T lymphocytes and M2 macrophages¹ considering, among other hypotheses, the properties of immune cells and their role in tumor progression. Sahoo et al. [15], developed a mathematical model based on prey-predator dynamics to explore the kinetics of CAR T-cells in a solid tumor (glioma). Their findings revealed that the death rate of CAR T-cells has a direct relationship with the proliferation rate and exhaustion. This suggests that lower doses of immunotherapy treatment are more effective, even though these cells become more exhausted compared to higher doses of treatment. The interaction between tumor cells, effector, and memory CAR T-cells was explored in a mathematical model, as documented in the studies by Barros et al. and Paixão et al. [2, 11]. One key goal of these studies was to assess the long-term role of memory CAR T-cells in fighting haematological tumors.

Considering the challenges of using CAR T-cell immunotherapy against cutaneous melanoma, the present work aims to develop a mathematical model based on Ordinary Differential Equations

¹Tumor-Associated Macrophages are also called M2-type macrophages.

(ODE) to describe the tumor dynamics of advanced melanoma considering its immunosuppressive TME in the presence of TAM, as well as answer the question: What are the underlying factors contributing to the ineffectiveness of CAR T-cell therapy in combatting melanoma, and what is the influence of TAM in this therapeutic failure?

This paper is structured as follows: In Section 2, we present the proposed mathematical model based on ODE and describe its variables and parameters. Furthermore, we present the equilibrium points and the linear stability analysis. In Section 3 we present the sensitivity analysis and simulations considering some scenarios. Finally, in Section 4, we end this paper with conclusions.

2 MATHEMATICAL MODEL

Based on previous works [2, 4, 15], we formulated an ODE model describing the interactions between melanoma cells (T), TAM (M) and CAR T-cells (C) as a function of time t , defined as follows:

$$\left\{ \begin{array}{l} \frac{dT}{dt} = \underbrace{\alpha_1 T \left(1 - \frac{T}{K_1}\right)}_{A_1} (1 + \beta_1 M) - \underbrace{\mu_1 CT}_{A_2}, \\ \frac{dM}{dt} = \underbrace{\alpha_2 MT \left(1 - \frac{M}{K_2}\right)}_{A_3} - \underbrace{\kappa_2 M}_{A_4}, \\ \frac{dC}{dt} = \underbrace{\alpha_3 CT}_{A_5} - \underbrace{\gamma_3 CT}_{A_6} - \underbrace{\theta_3 MC}_{A_7} - \underbrace{\kappa_3 C}_{A_8}. \end{array} \right. \quad (2.1)$$

The model incorporates several key biological assumptions:

- In the first equation, the term A_1 accounts for tumor growth according to a logistic growth model, in addition to representing the influence of TAM on tumor progression. TAM are known to promote tumor advancement through the secretion of various biological factors, including growth factors, pro-angiogenic molecules, and immunosuppressive agents such as IL-10, as supported by previous studies [20, 22]. Furthermore, the A_2 term assumes that CAR T-cells are effective in the elimination of melanoma cells by recognizing specific antigens such as CD126, MCSP, VEGFR2, GD2, and others, as indicated in the literature [2, 13, 19].
- In the second equation, the term A_3 , captures the phenomenon of TAM infiltration into the TME, responding to the presence of cytokines and chemokines produced by melanoma cells. This term further encompasses the population dynamics of TAM, characterized by logistic growth, and takes into account their competition with melanoma cells up to a specified carrying capacity. Additionally, the term A_4 represents the contribution of natural death in the TAM population [4].
- In the third equation, the term A_5 , represents that the expansion of CAR T-cells is primarily governed by their interaction with tumor antigens, while the term A_6 posits that CAR-T

cells are susceptible to inhibition and exhaustion due to the presence of immunosuppressive mechanisms in the TME. These mechanisms arise from both melanoma cells and TAM, ultimately resulting in CAR T-cell exhaustion. Our primary focus is to understand the reasons underlying the ineffectiveness of CAR T-cell immunotherapy in melanoma treatment and to elucidate the role played by TAM in this ineffectiveness. Consequently, we have introduced the A_7 term to simulate the *in silico* impact of TAM on the CAR T-cell population. Additionally, the A_8 term is integrated into the model to represent the immunosuppressive nature of the TME in the context of melanoma.

Table 1 shows the parameters with their respective values and units, and the initial conditions.

Table 1: Descriptions, values and units of the parameters.

Parameter	Description	Value	Unit	Reference
α_1	Natural rate of tumor cells proliferation	0.69	day ⁻¹	[4]
α_2	Rate of macrophage proliferation promoted by the tumor	10^{-7}	(cells·day) ⁻¹	[4]
α_3	Proliferation rate of CAR T-cells due to contact with tumor antigen	$5 \cdot 10^{-8}$	(cells·day) ⁻¹	Assumed
β_1	Tumor proliferation rate due to pro-tumor action of TAM	$2.3 \cdot 10^{-10}$	cells ⁻¹	[4]
K_1	Tumor cell carrying capacity	10^9	cells	[4]
K_2	Macrophage carrying capacity	10^9	cells	[4]
μ_1	Tumor cell death rate due to cytotoxic action of CAR T-cells	$[10^{-7}, 10^{-6}]$	(cells·day) ⁻¹	Assumed
κ_2	Macrophage apoptosis rate	0.34	day ⁻¹	[4]
γ_3	CAR T-cells immunosuppression rate caused by melanoma cells	$4 \cdot 10^{-8}$	(cells·day) ⁻¹	Assumed
θ_3	CAR T-cells immunosuppression rate caused by TAM	$[0, 5 \cdot 10^{-10}]$	(cells·day) ⁻¹	Assumed
κ_3	CAR T-cells apoptosis rate	[0.1, 0.5]	day ⁻¹	Assumed
$T(0)$	Initial condition of the tumor cells	$[2.5 \cdot 10^5, 5 \cdot 10^6]$	cells	Assumed
$M(0)$	Initial condition of the TAM	10^6	cells	[20]
$C(0)$	Initial condition of the CAR T-cells	$[2.5 \cdot 10^5, 5 \cdot 10^6]$	cells	Assumed

We set the initial condition $T(0)$ to model advanced-stage melanoma, justifying the use of CAR-T immunotherapy. $M(0)$ represents the TAM percentage in the TME, which can reach 50% in solid tumors like melanoma [20]. $C(0)$ is based on Barros et al. and Leon-Triana et al., and represents the immunotherapeutic dose of CAR T-cells injected into the tumor [2, 7]. The rationale for the parameters values presented in Table 1 are explained as follows:

- α_3 : describes the rate of stimulation of CAR-T cell proliferation due to the recognition of the tumor antigen. This parameter is related to the CAR product and was taken from Barros et al. [2] that estimated values are between $4.5 \cdot 10^{-8}$ and $1.23 \cdot 10^{-8}$ (cell·day)⁻¹.
- μ_1 : represents the CAR T-cell cytotoxicity. Based on the work of Barros et al. (2021) [2], the estimated the cytotoxic efficiency of CAR-T cells is in a range between $3.36 \cdot 10^{-8}$ and $3.71 \cdot 10^{-6}$ (cell·day)⁻¹.

- γ_3 : denotes the CAR T-cells TAM-induced immunosuppression rate. This parameter was selected under the assumption that the exhaustion rate of CAR-T cells is lower than the expansion rate (α_3).
- θ_3 : characterizes the interaction of CAR-T cells with immunosuppressive factors produced by TAM in the TME, for instance, the programmed death protein PD-1 [18, 19]. As experimental measurements are not available for this kinetic parameter, the value was assumed in the range $[0, 5 \cdot 10^{-10}]$ (cell·day) $^{-1}$ in order to simulate such phenomena.
- κ_3 : describes the apoptosis rate of CAR T-cells. This parameter considered Barros et al. [2], observations that the population of CAR-T cells decreases at a rate that includes natural death, along with other factors, and the mortality parameter adjusted to data available in the literature was 0.3 day^{-1} . Building upon this work, the parameter value was selected within an interval of $[0.1, 0.5] \text{ day}^{-1}$, encompassing the estimated value in [2].

2.1 Equilibrium points

Without loss of generality, let us consider $\alpha_3 - \gamma_3 = \beta_3$. The equilibrium points can be found from the solution of the following system of equations:

$$\begin{cases} \left(\alpha_1 \left(1 - \frac{T^*}{K_1} \right) (1 + \beta_1 M^*) - \mu_1 C^* \right) T^* = 0, \\ \left(\alpha_2 T^* \left(1 - \frac{M^*}{K_2} \right) - \kappa_2 \right) M^* = 0, \\ (\beta_3 T^* - \theta_3 M^* - \kappa_3) C^* = 0. \end{cases} \quad (2.2)$$

Considering that cell populations cannot be negative, the equilibrium points and their respective biological meanings are:

- $E_0 = (0, 0, 0)$. The trivial equilibrium point, which is not biologically relevant, since it represents the extinction of all cell populations.
- $E_1 = (K_1, 0, 0)$. This equilibrium point represents the failure of immunotherapy treatment and describes the persistence of melanoma cells up to the carrying capacity K_1 . In addition, disappearance of CAR T-cells and TAM population occurs.
- $E_2 = \left(K_1, K_2 \left(1 - \frac{\kappa_2}{\alpha_2 K_1} \right), 0 \right)$ which will have biological significance if $\alpha_2 \geq \kappa_2 / K_1$. As the equilibrium point E_2 , this also represents the failure of immunotherapeutic treatment, in which the disappearance of CAR T-cells and the persistence of the macrophage population occurs. Furthermore, this equilibrium point intersects E_1 when $\alpha_2 = \kappa_2 / K_1$.

- $E_3 = \left(\frac{\kappa_3}{\beta_3}, 0, \frac{\alpha_1}{\mu_1} \left(1 - \frac{\kappa_3}{\beta_3 K_1} \right) \right)$ which will have biological significance if $\beta_3 \geq \kappa_3/K_1$. This point represents the disappearance of the TAM population and the persistence of melanoma cells and CAR T-cells, and equals E_1 when $\beta_3 = \kappa_3/K_1$.

- The state of coexistence satisfies:

$$\begin{cases} \alpha_1 \left(1 - \frac{T^*}{K_1} \right) (1 + \beta_1 M^*) - \mu_1 C^* = 0, \\ \alpha_2 T^* \left(1 - \frac{M^*}{K_2} \right) - \kappa_2 = 0, \\ \beta_3 T^* - \theta_3 M^* - \kappa_3 = 0. \end{cases} \tag{2.3}$$

From the third equation of (2.3), let M^* be expressed in terms of T^* , such that

$$M^* = \frac{\beta_3 T^* - \kappa_3}{\theta_3}. \tag{2.4}$$

Substituting (2.4) into the second equation of (2.3), we have

$$\alpha_2 T^* \left(1 - \frac{T^* \beta_3 - \kappa_3}{\theta_3 K_2} \right) - \kappa_2 = 0, \tag{2.5}$$

with the roots

$$T_1^* = \frac{\alpha_2 (K_2 \theta_3 + \kappa_3) + \sqrt{\delta}}{2\alpha_2 \beta_3} \text{ and } T_2^* = \frac{\alpha_2 (K_2 \theta_3 + \kappa_3) - \sqrt{\delta}}{2\alpha_2 \beta_3}, \tag{2.6}$$

where

$$\delta = \alpha_2 (K_2^2 \alpha_2 \theta_3^2 + 2K_2 \alpha_2 \kappa_3 \theta_3 - 4K_2 \beta_3 \kappa_2 \theta_3 + \alpha_2 \kappa_3^2). \tag{2.7}$$

Given that $\beta_3 = \alpha_3 - \gamma_3$, for $T_{1,2}^* \in \mathbb{R}$, the following condition must be satisfied

$$\delta \geq 0 \Rightarrow \alpha_3 \leq \frac{\alpha_2 (K_2^2 \theta_3^2 + 2K_2 \kappa_3 \theta_3 + \kappa_3^2)}{4K_2 \kappa_2 \theta_3} + \gamma_3. \tag{2.8}$$

In the analysis of the component T_1^* from equation (2.6), when considering a given set of parameters, if $\delta \geq 0$, then the condition $T_1^* \geq 0$ is satisfied if:

$$\frac{\alpha_2 (K_2 \theta_3 + \kappa_3) + \sqrt{\delta}}{2\alpha_2 \beta_3} \geq 0 \Rightarrow -4K_2 \beta_3 \kappa_2 \theta_3 \leq 0 \Rightarrow \beta_3 \geq 0. \tag{2.9}$$

The condition $\beta_3 \geq 0$ implies that $\alpha_3 \geq \gamma_3$. From a biological perspective, this means that for $T_1^* \geq 0$, the proliferation rate of CAR-T cells due to interaction with the tumor antigen must exceed the immunosuppression rate induced by the tumor cells.

Analyzing $T_2^* \geq 0$ from equation (2.6) in terms of $\beta_3 = \alpha_3 - \gamma_3$, the condition to be satisfied is

$$\frac{\alpha_2(K_2\theta_3 + \kappa_3) - \sqrt{\delta}}{2\alpha_2\beta_3} \geq 0 \Rightarrow -4K_2\beta_3\kappa_2\theta_3 \geq 0 \Rightarrow \beta_3 \leq 0 \Rightarrow \alpha_3 \leq \gamma_3. \quad (2.10)$$

If $\beta_3 \leq 0$, this implies that $\alpha_3 \leq \gamma_3$. Consequently, for $T_2^* \geq 0$ to hold, the proliferation rate of CAR-T cells must be lower than the rate of immunosuppression caused by the tumor cells. In terms of treatment, the equilibrium point E_2^* lacks significance, as CAR-T cell proliferation will always outweigh immunosuppression. Therefore, these findings suggest that the biological interpretation of components T_1^* and T_2^* may depend on the choices of parameters α_3 and γ_3 , with T_1^* assuming greater importance from a therapeutic perspective.

Then, substituting the coordinate T_1 from equation (2.6) in equation (2.4) to find M_1^* , we have

$$M_1^* = \frac{\alpha_2(K_2\theta_3 - \kappa_3) + \sqrt{\delta}}{2\alpha_2\theta_3}. \quad (2.11)$$

For M_1^* to have biological significance, it is necessary that $M_1^* \geq 0$. Therefore, since the $\beta_3 = \alpha_3 - \gamma_3$ and utilizing equation (2.7), we have that

$$\frac{\alpha_2(K_2\theta_3 - \kappa_3) + \sqrt{\delta}}{2\alpha_2\theta_3} \geq 0 \Rightarrow \beta_3\kappa_2 \leq \alpha_2\kappa_3 \Rightarrow \alpha_3 \leq \frac{\alpha_2\kappa_3}{\kappa_2} + \gamma_3. \quad (2.12)$$

Let us now consider the coordinate M_2^* . Substituting the coordinate T_2 from (2.6) in equation (2.4), we have that

$$M_2^* = \frac{\alpha_2(K_2\theta_3 - \kappa_3) - \sqrt{\delta}}{2\alpha_2\theta_3}. \quad (2.13)$$

In order for M_2^* to have biological significance, it is required that $M_2^* \geq 0$ that is,

$$\frac{\alpha_2(K_2\theta_3 - \kappa_3) - \sqrt{\delta}}{2\alpha_2\theta_3} \geq 0 \Rightarrow \beta_3\kappa_2 \geq \alpha_2\kappa_3 \Rightarrow \alpha_3 \geq \frac{\alpha_2\kappa_3}{\kappa_2} + \gamma_3. \quad (2.14)$$

We can note that if $\alpha_3 \geq \frac{\alpha_2\kappa_3}{\kappa_2} + \gamma_3$, then $T_2^* \leq 0$, and hence, E_2^* lacks biological significance.

From the first equation of (2.3), the C^* coordinate can be expressed in terms of T^* . Then

$$C^* = \frac{\alpha_1}{\mu_1} \left(1 - \frac{T^*}{K_1} \right) (1 + \beta_1 M^*). \quad (2.15)$$

The coexistence equilibrium point with biological significance is $E_1^* = E^*$. Then, assuming $T_1^* = T^*$, $M_1^* = M^*$, the coexistence equilibrium point is given by

$$E^* = \left(T^*, M^*, \frac{\alpha_1}{\mu_1} \left(1 - \frac{T^*}{K_1} \right) (1 + \beta_1 M^*) \right), \gamma_3 \leq \alpha_3 \leq \frac{\alpha_2\kappa_3}{\kappa_2} + \gamma_3. \quad (2.16)$$

2.2 Stability analysis

To analyze the equilibrium points stability, we assume that $\bar{E} = (\bar{T}, \bar{M}, \bar{C})$ represents any equilibrium point of the system (2.1). The Jacobian matrix associated with the system (2.1) is given by:

$$J = \begin{pmatrix} \frac{-2(\bar{M}\beta_1+1)(\bar{T}-\frac{\kappa_1}{\alpha_2})\alpha_1-\mu_1\bar{C}K_1}{K_1} & \frac{\alpha_1\bar{T}(K_1-\bar{T})\beta_1}{K_1} & -\mu_1\bar{T} \\ \frac{\alpha_2\bar{M}(K_2-\bar{M})}{K_2} & \frac{(\alpha_2\bar{T}-\kappa_2)K_2-2\alpha_2\bar{M}\bar{T}}{K_2} & 0 \\ \bar{C}\beta_3 & -\bar{C}\theta_3 & -\bar{M}\theta_3 + \bar{T}\beta_3 - \kappa_3 \end{pmatrix}.$$

The Jacobian matrix J associated to the equilibrium point $E_0 = (0, 0, 0)$ is given by

$$J_0 = \begin{pmatrix} \alpha_1 & 0 & 0 \\ 0 & -\kappa_2 & 0 \\ 0 & 0 & -\kappa_3 \end{pmatrix}. \tag{2.17}$$

The eigenvalues are $\lambda_1 = \alpha_1$, $\lambda_2 = -\kappa_2$ and $\lambda_3 = -\kappa_3$ and then the equilibrium point E_0 is unstable (saddle point).

As previously performed, the eigenvalues associated with Jacobian matrix J , evaluated in the equilibrium point $E_1 = (K_1, 0, 0)$ are $\lambda_1 = -\alpha_1$, $\lambda_2 = K_1\alpha_2 - \kappa_2$, and $\lambda_3 = K_1\beta_3 - \kappa_3$. Since that $\beta_3 = \alpha_3 - \gamma_3$, we can conclude that the equilibrium point E_1 is linearly asymptotically stable if, and only if, $\alpha_2 < \kappa_2/K_1$ and $\alpha_3 < (\kappa_3/K_1) + \gamma_3$.

Let us now consider the equilibrium point $E_2 = \left(K_1, K_2 \left(1 - \frac{\kappa_2}{\alpha_2 K_1}\right), 0\right)$, $\alpha_2 > \kappa_2/K_1$. The determinant of the Jacobian matrix J evaluated at the point E_2 yields the characteristic equation expressed as $(\lambda - a_{11})(\lambda - a_{22})(\lambda - a_{33}) = 0$, where a_{11} , a_{22} , and a_{33} are coefficients associated with the linearization of the dynamical system. The eigenvalues are given by $\lambda_1 = a_{11}$, $\lambda_2 = a_{22}$ and $\lambda_3 = a_{33}$. Then, since that $\beta_3 = \alpha_3 - \gamma_3$, the equilibrium point E_2 will be linearly asymptotically stable if

$$\begin{aligned} \lambda_1 < 0 &\Rightarrow \alpha_2 > \frac{K_2\beta_1\kappa_2}{K_1(K_2\beta_1+1)}, \quad \lambda_2 < 0 \Rightarrow \alpha_2 > \frac{\kappa_2}{K_1}, \text{ and} \\ \lambda_3 < 0 &\Rightarrow \alpha_3 < \frac{K_2\theta_3}{K_1} \left(1 - \frac{\kappa_2}{K_1\alpha_2}\right) + \gamma_3 + \frac{\kappa_3}{K_1}. \end{aligned} \tag{2.18}$$

Considering the equilibrium point $E_3 = \left(\frac{\kappa_3}{\beta_3}, 0, \frac{\alpha_1}{\mu_1} \left(1 - \frac{\kappa_3}{\beta_3 K_1}\right)\right)$, with $\beta_3 > \kappa_3/K_1$, the associated Jacobian matrix is given by

$$J_3 = \begin{pmatrix} b_{11} & b_{12} & b_{13} \\ 0 & b_{22} & 0 \\ b_{31} & b_{32} & 0 \end{pmatrix}, \tag{2.19}$$

where, $b_{11} = -\frac{\alpha_1 \kappa_3}{\beta_3 K_1}$, $b_{12} = \frac{\alpha_1 \kappa_3 \beta_1 (K_1 \beta_3 - \kappa_3)}{\beta_3^2 K_1}$, $b_{13} = -\frac{\mu_1 \kappa_3}{\beta_3}$, $b_{22} = \frac{\alpha_2 \kappa_3}{\beta_3} - \kappa_2$, $b_{31} = \frac{\alpha_1 (K_1 \beta_3 - \kappa_3)}{\mu_1 K_1}$ and $b_{32} = -\frac{\alpha_1 \theta_3 (K_1 \beta_3 - \kappa_3)}{\mu_1 K_1 \beta_3}$. The characteristic equation associated to the Jacobian matrix (2.19) is given by

$$(\lambda - b_{22})(\lambda^2 - \lambda b_{11} - b_{13} b_{31}) = 0. \tag{2.20}$$

Since that $\beta_3 = \alpha_3 - \gamma_3$, from the first term of (2.20), we have that $\lambda_1 = b_{22}$. It is negative if

$$\alpha_3 > \frac{\alpha_2 \kappa_3}{\kappa_2} + \gamma_3. \tag{2.21}$$

For the second term of (2.20), we use the Routh-Hurwitz criterion:

- $p_1 = -b_{11} > 0$, then we have that

$$-\left(-\frac{\alpha_1 \kappa_3}{\beta_3 K_1}\right) > 0 \Rightarrow \frac{\alpha_1 \kappa_3}{(\alpha_3 - \gamma_3) K_1} > 0 \Rightarrow \alpha_3 > \gamma_3. \tag{2.22}$$

- $p_2 = -b_{13} b_{31} > 0 \Rightarrow \kappa_3 \alpha_1 \left(1 - \frac{\kappa_3}{\beta_3 K_1}\right) > 0$ and, it is satisfied if

$$\beta_3 > \frac{\kappa_3}{K_1} \Rightarrow \alpha_3 > \frac{\kappa_3}{K_1} + \gamma_3. \tag{2.23}$$

Therefore, if the above conditions are satisfied, the equilibrium point E_3 is stable.

Let us analyse the coexistence equilibrium point $E^* = (T^*, M^*, C^*)$, with $\alpha_3 \geq \gamma_3$, $\alpha_3 \leq \frac{\alpha_2 \kappa_3}{\kappa_2} + \gamma_3$, where T^* , M^* and C^* given by equations (2.6), (2.4) and (2.15), respectively. The Jacobian matrix is expressed by

$$J^* = \begin{pmatrix} c_{11} & c_{12} & c_{13} \\ c_{21} & c_{22} & 0 \\ c_{31} & c_{32} & 0 \end{pmatrix}, \tag{2.24}$$

where

$$\begin{aligned} c_{11} &= -\frac{\alpha_1 T^*}{K_1} (1 + M^*), & c_{12} &= \alpha_1 \beta_1 T^* \left(1 - \frac{T^*}{K_1}\right), & c_{13} &= -\mu_1 T^*, \\ c_{21} &= \alpha_2 M^* \left(1 - \frac{M^*}{K_2}\right), & c_{22} &= \alpha_2 T^* \left(1 - \frac{2M^*}{K_2}\right) - \kappa_2, \\ c_{31} &= \frac{\alpha_1 \beta_3}{\mu_1} \left(1 - \frac{T^*}{K_1}\right) (1 + \beta_1 M^*), & c_{32} &= -\frac{\alpha_1 \theta_3}{\mu_1} \left(1 - \frac{T^*}{K_1}\right) (1 + \beta_1 M^*). \end{aligned}$$

Then, the characteristic equation associated to the matrix (2.24) is given by $\lambda^3 + q_1 \lambda^2 + q_2 \lambda + q_3 = 0$, with $q_1 = -(c_{11} + c_{22})$, $q_2 = c_{11} c_{22} - c_{12} c_{21} - c_{13} c_{31}$ and $q_3 = c_{13} c_{21} c_{32} + c_{13} c_{22} c_{31}$. We can apply the Routh-Hurwitz criterion to assess the stability of the E^* coexistence equilibrium point. However, analyzing the stability of the coexistent state (T^*, M^*, C^*) is more challenging when considering all model parameters. Consequently, we utilize the parameters values presented in Table 1 to determine the equilibrium points and their respective stability.

The conditions for the existence and stability of equilibrium points E_i^* , $i = 1, 2, 3$, as well as the coexistence equilibrium point E^* , are dependent on the parameter α_3 . In particular, it is worth noting that eventually, such conditions are expressed in terms of α_2 . Then, given the parameters presented in Table 1, we conducted variations in the parameter α_2 to analyze the stability and existence of equilibrium points, as presented in Table 2.

Table 2: Stability analysis with variations in the parameter α_2 .

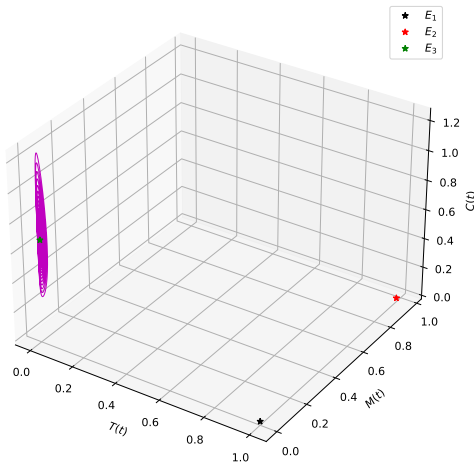
	$\alpha_2 = 10^{-8}$	$\alpha_2 = 1.777 \cdot 10^{-8}$	$\alpha_2 = 2.555 \cdot 10^{-8}$	$\alpha_2 = 3.333 \cdot 10^{-8}$
E_1	Unstable	Unstable	Unstable	Unstable
E_2	Unstable	Unstable	Unstable	Unstable
E_3	Stable spiral	Stable spiral	Stable spiral	Unstable spiral
E^*	Does not exist	Does not exist	Does not exist	Stable spiral
	$\alpha_2 = 4.888 \cdot 10^{-8}$	$\alpha_2 = 5.666 \cdot 10^{-8}$	$\alpha_2 = 6.444 \cdot 10^{-8}$	$\alpha_2 = 8 \cdot 10^{-8}$
E_1	Unstable	Unstable	Unstable	Unstable
E_2	Unstable	Unstable	Unstable	Unstable
E_3	Unstable spiral	Unstable spiral	Unstable spiral	Unstable spiral
E^*	Stable spiral	Stable spiral	Stable spiral	Stable spiral

It is possible to observe that, for the first three chosen values of α_2 , the coexistence point E^* does not exist, meaning the existence condition imposed in equation (2.7) is not met (the point belongs to the set of complex numbers), and thus the equilibrium point E_3 is a stable spiral. When the parameter α_2 increases, the existence condition for the equilibrium point E^* is satisfied, and it stabilizes into a stable spiral.

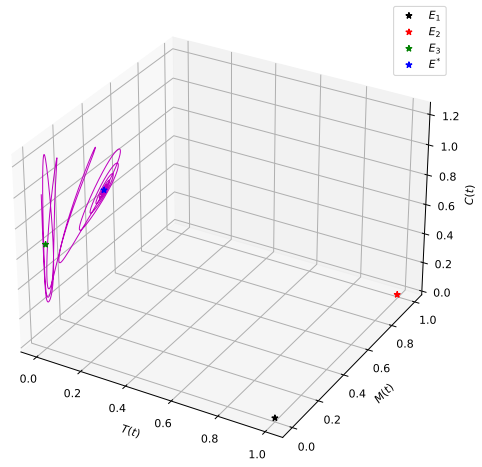
To graphically analyze the results presented in Table 2, we conducted numerical simulations using the parameters listed in Table 1 and selected four specific values for α_2 , defined as, $\alpha_2 = 10^{-8}$, $\alpha_2 = 3.333 \cdot 10^{-8}$, $\alpha_2 = 4.888 \cdot 10^{-8}$, and $\alpha_2 = 8 \cdot 10^{-8}$ (cell·day)⁻¹. The initial conditions were set as $T(0) = 2 \cdot 10^6$, $M(0) = 10^6$, and $C(0) = 10^7$ cells. The results are illustrated in Figure 1.

Figure 1 shows that as α_2 increases, equilibrium point E_3 loses stability, giving rise to coexistence point E^* , which stabilizes as a stable spiral. Furthermore, in Figure 1(d), when $\alpha_2 = 4.888 \cdot 10^{-8}$ (cells·day)⁻¹, the solution orbits around equilibrium point E^* , indicating the presence of a limit cycle.

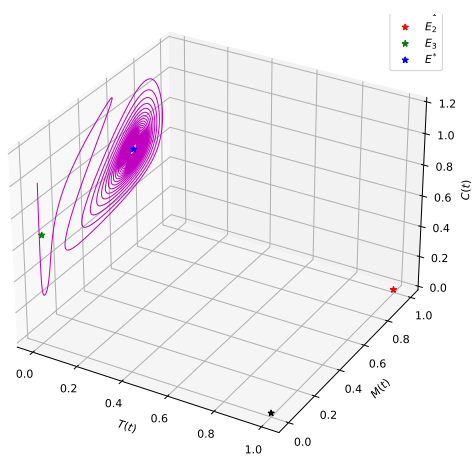
From a biological perspective, when tumor-promoted TAM proliferation increases alongside a relatively high CAR-T cell proliferation rate ($\alpha_2 = 5 \cdot 10^{-8}$ (cell·day)⁻¹), it tends to support the



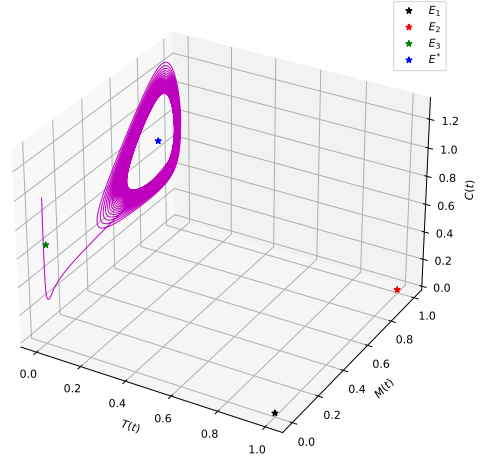
(a) $\alpha_2 = 10^{-8}$ (cell-day).



(b) $\alpha_2 = 3.333 \cdot 10^{-8}$ (cell-day).



(c) $\alpha_2 = 4.888 \cdot 10^{-8}$ (cell-day).



(d) $\alpha_2 = 8 \cdot 10^{-8}$ (cell-day).

Figure 1: Stability analysis with variations in the parameter α_2 , considering $T(0) = 2 \cdot 10^6$ cells, $M(0) = 10^6$ cells, and $C(0) = 10^7$ cells. The black, red, green, and blue stars represent equilibrium points E_1 , E_2 , E_3 , and E^* , respectively. An increase in the proliferation rate of TAM contributes to the stability of the coexistence equilibrium point E^* .

coexistence of these cells. Conversely, when macrophage proliferation is low, potentially due to drugs shifting pro-tumor toward an anti-tumor macrophage phenotype, it enables coexistence between tumor cells and CAR-T cells, which is advantageous for treatment.

3 RESULTS AND DISCUSSIONS

Several models, focusing on CAR T-cell kinetics, were developed to illustrate its distinct phases, including distribution, expansion, contraction, and persistence. In the contraction and persistence phase, effector CAR-T cells experience activation-induced cell death (AICD), resulting in a reduced population. While CAR-T cells might change their phenotype during this phase, such as transitioning into memory CAR-T cells that persist longer and contribute to the immune response against cancer, this study primarily focuses on effector CAR-T cells, which are not circulating after the contraction phase [12].

To adapt the simulations for a realistic scenario, such as when effector CAR T-cells are exhausted or the tumor loses antigen, we used a numerical procedure² that the CAR T-cells population will not re-expand even if the tumor escapes. The numerical procedure involves the implementation of an adapted fourth-order Runge-Kutta method ensuring that, following the contraction phase, effector CAR-T cells will not re-expand. In other words, once the population reaches its lowest point after the expansion peak, it becomes fixed at that minimum level. Furthermore, we defined tumor control as the duration during which the tumor population T stays below 10^2 cells [2].

The simulations were performed by implementing the adapted algorithm in Python. The parameter values used in the numerical simulations are listed in Table 1, and the time step employed in the method was $h = 0.01$ with a simulation period of $t = 80$ days.

3.1 Sensitivity Analysis

The dynamics underlying CAR T-cell therapy are recognized to be the result of an interplay of many phenomena that occur at different biological populations; however, some indirect effects, such as cytokine production, the interaction of endogenous immune cells (macrophages, NK cells and so on) are not well understood, and many mechanisms remain unanswered.

The ODE system presented in Equations (2.1) has 10 parameters that have been considered from previous research. In models with several uncertain inputs, it is important to assess which parameters have a significant impact on the outputs. To this end, we perform a sensitivity analysis (SA) [16] using the elementary effects (EE) technique, by measuring the effect of small parameter changes (a perturbation of $\pm 25\%$ from the values established in Table 1) on different quantities of interest (QoI) of the model using an eighty-day simulation of the system's evolution, as well as the adapted algorithm.

On the EE method, the selected output of interest can be represented by a function $Y(\mathbf{X})$, where $\mathbf{X} = (X_1, \dots, X_d)$ is a vector of d independent input variables (parameters) defined within the range of a continuous interval. The elementary effect of the i -th input factor for a given value of \mathbf{X} is defined as:

$$EE_i = \frac{Y(X_1, \dots, X_i + \Delta, \dots, X_d) - Y(\mathbf{X})}{\Delta} = \frac{Y(\mathbf{X} + \mathbf{e}_i \Delta) - Y(\mathbf{X})}{\Delta}, \quad (3.1)$$

²Algorithms used are available at https://github.com/g-rodriques2/Algorithms_TCAM

where Δ is a predetermined perturbation factor of X_i and $Y(\mathbf{X} + \mathbf{e}_i\Delta)$ is the model output corresponding to a Δ change in X_i . The distribution of the elementary effects (ρ_i) for each input parameter is obtained by constructing r -trajectories in a grid of d -dimensions and p -levels, where each input is randomly sampled using a one-at-a-time (OAT) sampling strategy.

In order to rank the parameters, we chose to estimate the mean μ_i of the distribution (ρ_i). This measure evaluates the general impact of the i -th parameter on the output (QoI) and the average of absolute elementary effects is $\mu_i^* = \frac{1}{r} \sum_{j=1}^r |EE_i^j|$.

The results of this parameter sensitivity analysis for the mathematical model are shown in Figure 2. In the case where the QoI is the tumor load, Figure 2(a) shows that the system is found to be most sensitive to the balance between the CAR-T proliferation and inhibition rates ($\alpha_3 - \gamma_3$), as well as to the tumor growth parameter and its carrying capacity K_1 . This suggests that, in addition to the tumor's aggressiveness, as represented by growth parameter α_1 , even minor differences in the absolute number of CAR-T cells in the system during the dynamics can affect clinical outcome. It is possible to notice that, during tumor escape, all parameters associated with changes in CAR-T cell concentration appear to be relevant, including θ_3 and κ_3 . This would indicate that any treatment which might enhance CAR T-cell expansion should be pursued. By contrast, the size of the tumor after eighty days is not very sensitive to the TAM participation in tumor progression expressed by β_1 . According to this model, then, the pro-tumor action of TAM alone is not a determining factor in the eventual size of the tumor, and the cytolytic activity should be considered as the conjunction of number of CAR T-cells binding with tumor cells as well as its killing efficacy.

In the scenario where the output is the concentration of macrophages, Figure 2(b) shows that during an initial expansion phase, this population is highly sensitive to the TAM's intrinsic characteristics (α_2 and κ_2) together with tumor proliferation (α_1). Then, as the macrophage population is being depleted and similar to what was described previously for the tumor, the system is also sensitive to the balance between the CAR T-cell proliferation and inhibition rates ($\alpha_3 - \gamma_3$). This reveals that, while CAR T-cells do not directly interact with TAM, their action in reducing tumor population will have an indirect effect on the interplay between tumor cells and macrophages. Matter of fact, during tumor progression, TAM are again recruited to the tumor site, and CAR T-cells attempt to control these populations at first, but then these populations escape.

At last, when QoI is the CAR T-cell density, during an initial phase, the model is most sensitive to the CAR T expansion strength, given by antigen recognition ($\alpha_3 - \gamma_3$) and its natural apoptotic rate κ_3 . After the peak, during the contraction phase, the inhibition of CAR T-cells by macrophages (θ_3), and the absolute number of TAM in the microenvironment might affect the residual number of CAR T in the system. This finding, indicates that investigating CAR T-cell interactions with the host immune system could shed light on the mechanisms underlying (non)durable responses. The sensitivity analysis shows that, during the final phase, antigen binding and CAR T proliferation alone are not determining factors in CAR T-cell persistence, and its efficiency in killing tumor cells must also be considered.

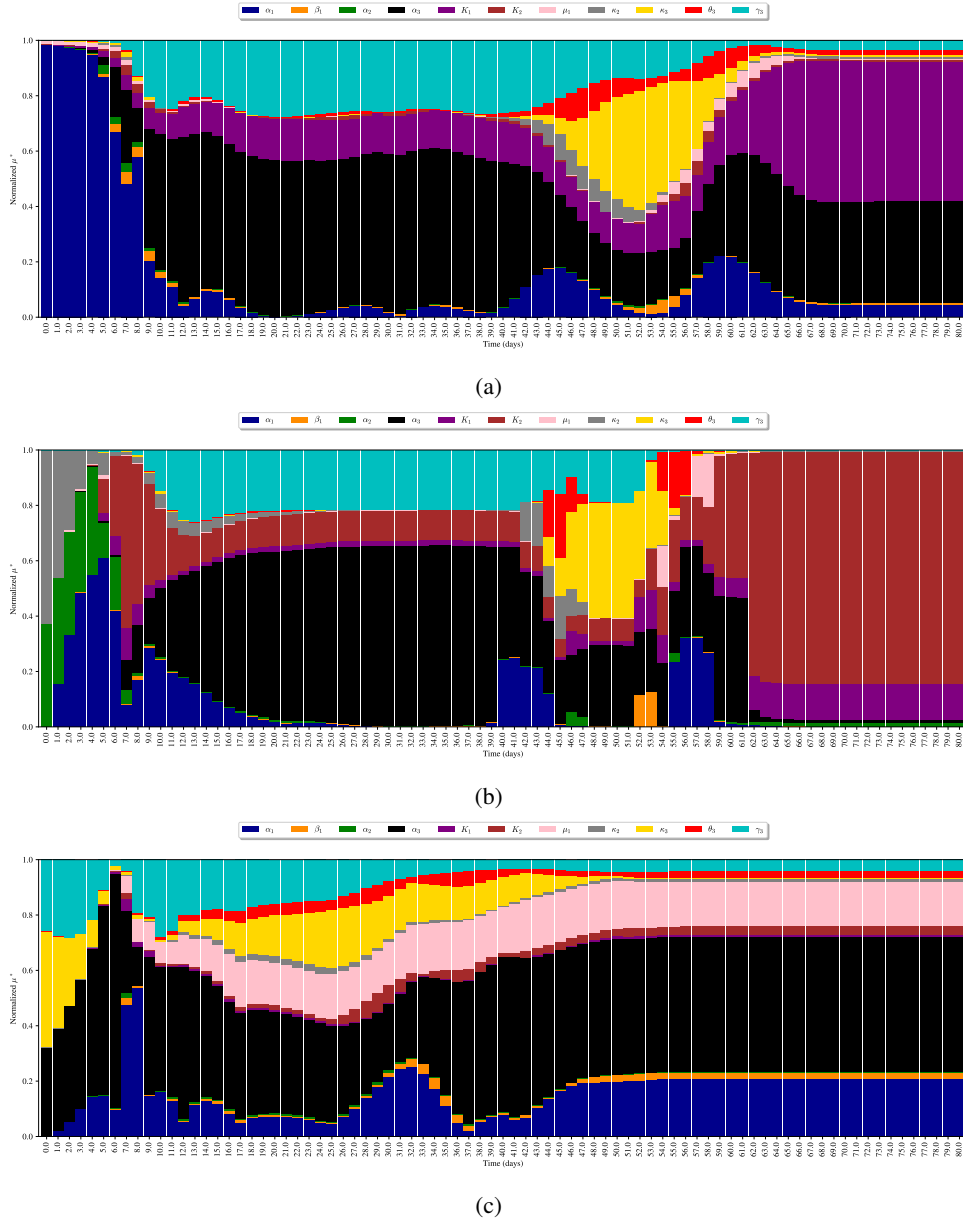


Figure 2: Sensitivity analysis was performed using the EE method for different quantities of interest (QoI) with $r = 40$ and $p = 4$. The average of absolute elementary effects is shown in (a) tumor/Melanoma Cells, (b) TAM population and (c) CAR T-cells. The parameters from Table 1 and $\theta_3 = 10^{-10}$ (cells·day) $^{-1}$ were perturbed by $\pm 25\%$ and the system’s evolution was simulated for eighty days.

3.2 Numerical Simulations

3.2.1 TAM inhibition affects tumor control

The immunosuppressive TME represents a major barrier to effective tumor-specific T-cell responses to cancer [14]. Since TAM are major constituents of the TME, and consist of a highly heterogeneous population, we first studied the impact caused by an increasingly immunosuppressive TME in a patient undergoing CAR T-cell therapy. In order to achieve this objective, we conducted a series of simulations in which where we varied the parameter θ_3 , as can be seen in Figure 3.

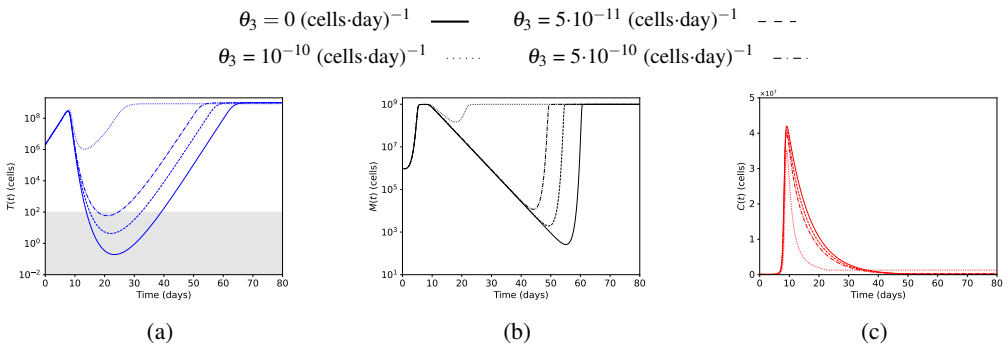


Figure 3: An immunosuppressive TME significantly impacts tumor control *in-silico*. Dynamics of the number of tumor cells (blue curves), TAM cells (black curves) and CAR T-cells (red curves) ruled by Equation (2.1) in different immunosuppression scenarios. Initial data used in the simulations $T(0) = 2 \cdot 10^6$ cells, $M(0) = 10^6$ cells and $C(0) = 5 \cdot 10^5$ cells and parameter values presented in Table 1. The grey shaded area represent the non-detection limit of 10^2 cells.

TAM-induced immunosuppression has a negative impact on treatment, as illustrated in Figure 3(a). It is possible to observe that in a highly immunosuppressive TME, the tumor is not controlled at all; however, in an environment where the immunosuppression is gradually decreasing, $\theta_3 = 5 \cdot 10^{-11}$, $\theta_3 = 10^{-10}$, $\theta_3 = 5 \cdot 10^{-10} \text{ (cells}\cdot\text{day)}^{-1}$, the tumor is controlled during 6, 17, and 25 days, respectively. The simulations agree with clinical observations that TAM’s action correlates with poor survival in many types of solid cancer. These observations also suggests that therapeutics strategies targeting TAM subsets should be explored, even if extends the window of opportunity for the application of other therapies.

Figure 3(b) shows that TAM dynamics is similar to that of as in the melanoma cells. This scenario is expected considering that TAM are recruited to the tumor site, promoting its progression. Consequently, the depletion of tumor cells due to immunotherapy also affects the TAM population. This implies that even if TAM do not express the target-antigen of CAR T-cells, the treatment indirectly influences the dynamics of this population.

In Figure 3(c), we observe that macrophages play a pivotal role in the development of effective immunotherapy, the simulations show that increasing immunosuppression caused by TAM

enhances CAR T-cells contraction, thereby, affecting treatment efficacy. Moreover, from the parameter set used, the model was able to capture the phases of expansion, contraction and persistence, indicating that the functional response of the model is adequate to describe the dynamics of CAR T-cells [12]. Furthermore, our results corroborate data regarding the TAM-induced immunosuppression in the context of CAR T-cell therapy [9, 14, 24].

3.2.2 Killing efficiency affects CAR-T dynamics

Next, we investigated the effect of the CAR T-cells dosage in the system’s dynamics, also considering its different cytotoxic rates when targeting the tumor antigen. To achieve this, we performed simulations of equations (2.1) and we found a dependence of the dynamics on the number of injected CAR T-cells. Results shown in Figure 4 present some examples for numbers of cells initially injected, ranging from $2.5 \cdot 10^5$ to $5 \cdot 10^6$ cells.

$C(0) = 2.5 \cdot 10^5$ cells — $C(0) = 5 \cdot 10^5$ cells - - - $C(0) = 2.5 \cdot 10^6$ cells - - - $C(0) = 5 \cdot 10^6$ cells ·····

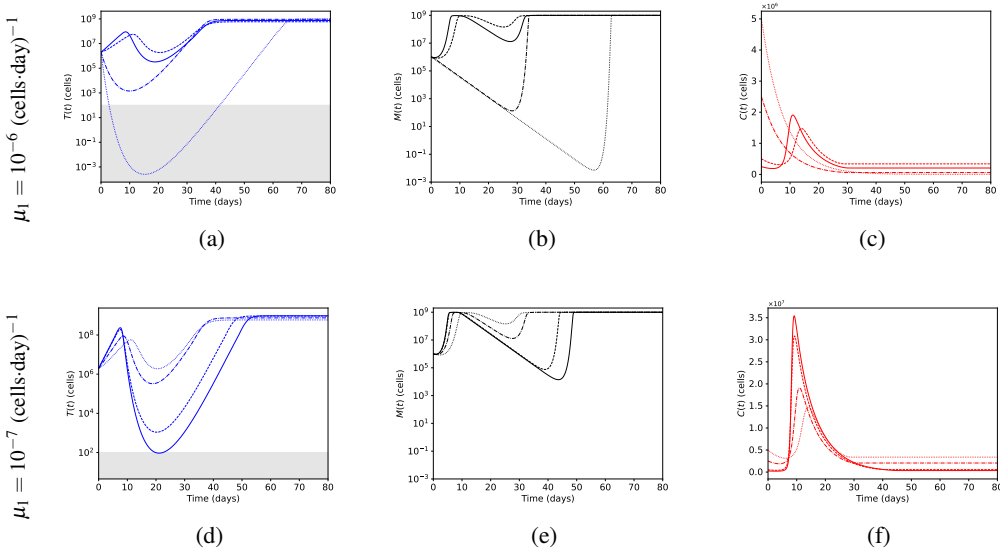


Figure 4: Killing efficiency and CAR T dose change the system dynamics. System evolution of the total number of tumor cells (blue curves), TAM cells (black curves) and CAR T-cells (red curves). The curves correspond to different values of CAR T-cells injected in a patient with initial tumor burden of $T(0) = 2 \cdot 10^6$ cells, $M(0) = 10^6$ cells. The parameter values used in the simulations are in Table 1 and $\theta_3 = 5 \cdot 10^{-11}$ (cells-day)⁻¹.

The top panel of Figure 4 shows two distinct dynamics in all populations, considering the initial dosage $C(0)$. Specifically for CAR T-cells, see Figure 4(c), a high cytotoxic rate ($\mu_1 = 10^{-6}$ (cell·day) $^{-1}$) promoted qualitative changes in the dynamics around $C(0) = 2.5 \cdot 10^6$ cells. Thus, small doses of CAR T-cells led to an early tumor progression followed by a small reduction in the tumor load (Figure 4(a)), while for larger doses, the therapy was able to control tumor growth for a longer period, a behavior also demonstrated by TAM (Figure 4(b)). Nevertheless, there is an apparent threshold related to the CAR-T dose and this particular set of parameters that promotes different outcomes and would change under different conditions, which may provide a durable response.

The bottom panel of Figure 4 shows a different dynamics when the cytotoxic activity against tumor is low ($\mu_1 = 10^{-7}$ (cell·day) $^{-1}$). The change in the magnitude of the initial CAR T-cell dose, had a significant effect on the maximum expansion achieved (Figure 4(c)). For our *in silico* simulations, a reduction in the efficiency of stimulation in the CAR T-cells led to a slower growth of this population. Since CAR T expansion relies on the contact with tumor cells, Figure 4(a) shows that a higher CAR T infusion, quickly decrease the tumor population which impairs CAR T levels on the system.

3.2.3 Initial tumor burden and CAR T interaction with antigen changes the overall dynamics

The initial tumor load on has a dual role: a high tumor load may favour the initial expansion of CAR T-cells on one hand, but it may enhance tumor immune suppression capabilities on the other. As a result, the question of how to use CAR T-cell treatments in combination with other neoadjuvant therapies arises. To shed some light on the question, we computationally investigated the idea of using CAR T-cells after a partial surgical resection or a primary regimen of radiotherapy, which is a common scenario in the context of melanoma.

In Figure 5 we notice that during the first weeks of treatment, the reduction in initial tumor load resulted in an initial tumor progression, which delays the expansion phase of CAR T-cells and gradually recruits TAM to the tumor site. A higher tumor burden, on the other hand, shortens the duration of the CAR T distribution phase, keeping more CAR T-cells in the system and slowing the initial tumor proliferation. Since a lower number of tumor cells implies a lower density of CAR T-cells, the CAR-peak levels in this case scenario are smaller. However, following the CAR T contraction phase, the greater the tumor burden, the greater the concentration of CAR T-cells during the persistence phase.

It is important to notice that this behaviour is most probably due to the tumor aggressiveness and to the TAM support to tumor growth. These findings suggest that a new CAR structure, designed to reprogram the TME, might indirectly limit tumor progression. However, when making broad statements about specific responses to treatments, caution is necessary, and any quantitative data must be interpreted as one possibility, with further investigation required for a different set of parameters.

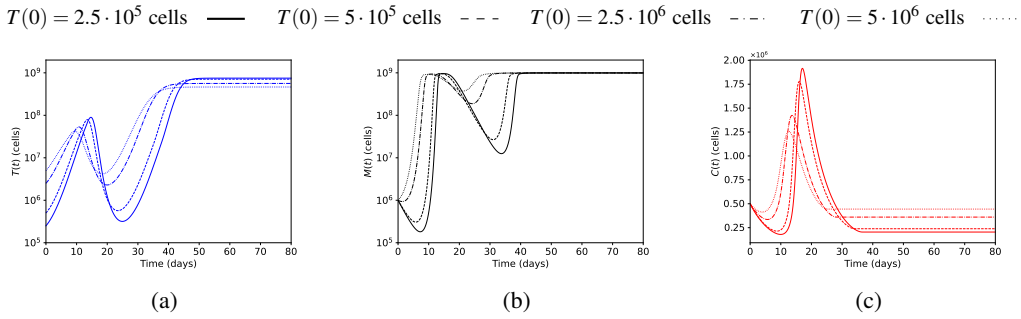


Figure 5: *In silico* simulations under different initial tumor loads. System evolution of the total number of tumor cells (blue curves), TAM cells (black curves) and CAR T-cells (red curves). The curves correspond to different values of tumor burden in a patient with initial CAR T injection of $C(0) = 5 \cdot 10^5$ cells, $M(0) = 10^6$ cells. The parameter values used in the simulations are in Table 1 and $\theta_3 = 5 \cdot 10^{-11}$ (cells·day)⁻¹.

4 CONCLUSIONS

From a proposed ODE model, it was possible to capture the expansion, contraction and persistence phases of CAR T-cells and their cytotoxic effects against cutaneous melanoma. The sensitivity analysis of the parameters showed that the pro-tumor action of TAM alone does not represent a determining factor for tumor growth. Furthermore, sensitivity analysis revealed that during the contraction phase of CAR T-cells the absolute number of TAM can affect the residual number of CAR T-cells in the system, revealing that interactions between CAR T-cells and immune system cells could shed light on the mechanisms that lead treatment to fail.

Analytical results and numerical simulations revealed the challenges for the applicability of CAR T-cell immunotherapy against melanoma. In the first scenario we investigated the inhibitory effects of TAM on CAR T-cells and the results showed that increased suppression inherent to TAM has a negative impact on treatment and, furthermore, our results corroborate clinical observations about poor survival of CAR T-cells in fighting several types of solid tumors, including melanoma. In the second scenario, we investigated the cytotoxic efficiency of CAR T-cells against melanoma and obtained as results that increasing the cytotoxicity of CAR T-cells in conjunction with initial immunotherapeutic dose adjustments may contribute to greater tumor control. Finally, in the third scenario we varied the initial tumor burden and found that this variation affects CAR T-cell dynamics in general, suggesting that the development of new CAR structures with the ability to reprogram the TME may be a strategy to limit tumor progression and increase immunotherapeutic efficacy. Indeed, the reasons why CAR T-cell therapy fails in fighting melanoma are many and our *in silico* analyses evidenced that TAM has an important role for this failure, opening the way for further investigations and improvements in therapeutic techniques.

Acknowledgments

This study was financed in part by the Coordenação de Aperfeiçoamento de Pessoal de Nível Superior – Brasil (CAPES) – Finance Code 001.

REFERENCES

- [1] M. Arnold, D. Singh, M. Laversanne, J. Vignat, S. Vaccarella, F. Meheus, A.E. Cust, E. de Vries, D.C. Whiteman & F. Bray. Global burden of cutaneous melanoma in 2020 and projections to 2040. *JAMA Dermatol.*, **158**(5) (2022), 495–503. doi:10.1001/jamadermatol.2022.0160.
- [2] L.R.C. Barros, E.A. Paixão, A.M.P. Valli, G.T. Naozuka, A.C. Fassoni & R.C. Almeida. CARTmath—A Mathematical Model of CAR-T Immunotherapy in Preclinical Studies of Hematological Cancers. *Cancers*, **13**(12) (2021). doi:10.3390/cancers13122941.
- [3] P. Chen, Y. Huang, R. Bong, Y. Ding, N. Song, X. Wang, X. Song & Y. Luo. Tumor-Associated Macrophages Promote Angiogenesis and Melanoma Growth via Adrenomedullin in a Paracrine and Autocrine Manner. *Clin. Cancer Res.*, **17**(23) (2011), 7230–7239. doi:10.1158/1078-0432.CCR-11-1354.
- [4] R. Eftimie & H. Hamam. Modelling and investigation of the CD4+ T cells – Macrophages paradox in melanoma immunotherapies. *J. Theor. Biol.*, **420** (2017), 82–104. doi:10.1016/j.jtbi.2017.02.022.
- [5] V. Gray-Schopfer, C. Wellbrock & R. Marais. Melanoma biology and new targeted therapy. *Nature*, **445**(7130) (2007), 851–857. doi:10.1038/nature05661.
- [6] Instituto Nacional do Câncer. Brasil - estimativa dos casos novos: Estimativas para o ano de 2023. Online (2022). URL <https://www.gov.br/inca/pt-br/assuntos/cancer/numeros/estimativa/estado-capital/brasil>. Accessed December 3, 2022.
- [7] O. León-Triana, A. Pérez-Martínez, M. Ramírez-Orellana & V.M. Pérez-García. Dual-Target CAR-Ts with On-and Off-Tumour Activity May Override Immune Suppression in Solid Cancers: A Mathematical Proof of Concept. *Cancers*, **13**(4) (2021), 703. doi:10.3390/cancers13040703.
- [8] A. Mantovani, F. Marchesi, A. Malesci, L. Laghi & P. Allavena. Tumour-associated macrophages as treatment targets in oncology. *Nat. Rev. Clin. Oncol.*, **14**(7) (2017), 399–416. doi:10.1038/nrclinonc.2016.217.
- [9] A.Z. Mehrabadi, R. Ranjbar, M. Farzanehpour, A. Shahriary, R. Dorostkar, M.A. Hamidinejad & H.E.G. Ghaleh. Therapeutic potential of CAR T cell in malignancies: A scoping review. *Biomed. Pharmacother.*, **146** (2022), 112512. doi:10.1016/j.biopha.2021.112512.
- [10] S.S. Mojsilovic, S. Mojsilovic, V.H. Villar & J.F. Santibanez. The Metabolic Features of Tumor-Associated Macrophages: Opportunities for Immunotherapy? *Anal. Cell. Pathol.*, **2021** (2021), 12. doi:10.1155/2021/5523055.
- [11] E.A. Paixão, L.R.C. Barros, A.C. Fassoni & R.C. Almeida. Modeling Patient-Specific CAR-T Cell Dynamics: Multiphasic Kinetics via Phenotypic Differentiation. *Cancers*, **14**(22) (2022). doi:10.3390/cancers14225576.

- [12] T. Qi, K. McGrath, R. Ranganathan, G. Dotti & Y. Cao. Cellular Kinetics: A Clinical and Computational Review of CAR-T Cell Pharmacology. *Adv. Drug Deliver. Rev.*, (2022), 114421. doi:10.1016/j.addr.2022.114421.
- [13] A. Razavi, M. Keshavarz-Fathi, J. Pawelek & N. Rezaei. Chimeric antigen receptor T-cell therapy for melanoma. *Expert Rev. Clin. Immunol.*, **17**(3) (2021), 209–223. URL <https://doi.org/10.1080/1744666X.2021.1880895>.
- [14] A. Rodriguez-Garcia, R.C. Lynn, M. Poussin, M.A. Eiva, L.C. Shaw, R.S. O'Connor, N.G. Minutolo, V. Casado-Medrano, G. Lopez, T. Matsuyama & D.J. Powell Jr. CAR-T cell-mediated depletion of immunosuppressive tumor-associated macrophages promotes endogenous antitumor immunity and augments adoptive immunotherapy. *Nat. Commun.*, **12**(1) (2021), 1–17.
- [15] P. Sahoo, X. Yang, D. Abler, D. Maestrini, V. Adhikarla, D. Frankhouser, H. Cho, V. Machuca, D. Wang, M. Barish, M. Gutova, S. Branciamore, C.E. Brown & R.C. Rockne. Mathematical deconvolution of CAR T-cell proliferation and exhaustion from real-time killing assay data. *J. R. Soc. Interface*, **17**(162) (2020), 20190734. doi:10.1098/rsif.2019.0734.
- [16] A. Saltelli, M. Ratto, T. Andres, F. Campolongo, J. Cariboni, D. Gatelli, M. Saisana & S. Tarantola. “Global sensitivity analysis: the primer”. John Wiley & Sons (2008).
- [17] M. Shen, Y. Du & Y. Ye. Tumor-associated macrophages, dendritic cells, and neutrophils: biological roles, crosstalk, and therapeutic relevance. *Med. Rev.*, **1**(2) (2021), 222–243. doi:10.1515/mr-2021-0014.
- [18] B. Simon & U. Uslu. CAR T-cell therapy in melanoma: A future success story? *Exp. Dermatol.*, **27**(12) (2018), 1315–1321. doi:10.1111/exd.13792.
- [19] T. Soltantoyeh, B. Akbari, A. Karimi, G.M. Chalbatani, N. Ghahri-Saremi, J. Hadjati, M.R. Hamblin & H.R. Mirzaei. Chimeric Antigen Receptor (CAR) T Cell Therapy for Metastatic Melanoma: Challenges and Road Ahead. *Cells*, **10**(6) (2021). doi:10.3390/cells10061450.
- [20] I. Vitale, G. Manic, L.M. Coussens, G. Kroemer & L. Galluzzi. Macrophages and Metabolism in the Tumor Microenvironment. *Cell Metab.*, **30**(1) (2019), 36–50. doi:10.1016/j.cmet.2019.06.001.
- [21] A.D. Waldman, J.M. Fritz & M.J. Lenardo. A guide to cancer immunotherapy: from T cell basic science to clinical practice. *Nat. Rev. Immunol.*, **20**(11) (2020), 651–668. URL <https://doi.org/10.1038/s41577-020-0306-5>.
- [22] T. Yamaguchi, S. Fushida, Y. Yamamoto, T. Tsukada, J. Kinoshita, K. Oyama, T. Miyashita, H. Tajima, I. Ninomiya, S. Munesue *et al.* Tumor-associated macrophages of the M2 phenotype contribute to progression in gastric cancer with peritoneal dissemination. *Gastric Cancer*, **19**(4) (2016), 1052–1065. URL <https://doi.org/10.1007/s10120-015-0579-8>.
- [23] Q. Yang, N. Guo, Y. Zhou, J. Chen, Q. Wei & M. Han. The role of tumor-associated macrophages (TAMs) in tumor progression and relevant advance in targeted therapy. *Acta Pharm. Sin. B.*, **10**(11) (2020), 2156–2170. doi:<https://doi.org/10.1016/j.apsb.2020.04.004>. SI: Tumor Microenvironment and Drug Delivery.

- [24] Z.Z. Zhang, T. Wang, X.F. Wang, Y.G. Zhang, S.X. Song & C.G. Ma. Improving the ability of CAR-T cells to hit solid tumors: Challenges and strategies. *Pharmacol. Res.*, **175** (2022), 106036. doi:10.1016/j.phrs.2021.106036.
- [25] Z. Zhao, Y. Chen, N.M. Francisco, Y. Zhang & M. Wu. The application of CAR T-cell therapy in hematological malignancies: advantages and challenges. *Acta Pharm. Sin. B.*, **8**(4) (2018), 539–551. doi:10.1016/j.apsb.2018.03.001.

How to cite

G. Rodrigues, J.G. Silva, D.S. Santurio & P.F.A. Mancera. A mathematical model to describe the melanoma dynamics under effects of macrophage inhibition and CAR T-cell therapy. *Trends in Computational and Applied Mathematics*, **25**(2024), e01734. doi: 10.5540/tcam.2024.025.e01734.

